

# The Effect of Bound Dineutrons upon BBN

James P. Kneller\* and Gail C. McLaughlin†

*Department of Physics, North Carolina State University, Raleigh, North Carolina 27695-8202*

(Dated: April 1, 2021)

We have examined the effects of a bound dineutron,  ${}^2\text{n}$ , upon big bang nucleosynthesis (BBN) as a function of its binding energy  $B_{2\text{n}}$ . We find a weakly bound dineutron has little impact but as  $B_{2\text{n}}$  increases its presence begins to alter the flow of free nucleons to helium-4. Due to this disruption, and in the absence of changes to other binding energies or fundamental constants, BBN sets a reliable upper limit of  $B_{2\text{n}} \lesssim 2.5$  MeV in order to maintain the agreement with the observations of the primordial helium-4 mass fraction and D/H abundance.

PACS numbers: 99.99

## I. INTRODUCTION

The concordance of the predicted synthesis of the lightest nuclei during the period immediately following the Big Bang with the observed primordial abundances presents us with a powerful probe of the state of the Universe during its earliest epochs. In addition to constraining standard cosmological parameters such as the density of baryons, the number of neutrino flavors and their degeneracy [1, 2, 3, 4, 5, 6, 7, 8, 9, 10, 11, 12, 13, 14, 15] BBN is sufficiently complex that one can also learn about such possibilities as Quintessence [16, 17, 18, 19], modifications of gravity [19, 20] or neutrino oscillations/mass/decay [21, 22, 23, 24, 25, 26, 27, 28, 29].

Perhaps the most intriguing use of BBN is in constraining the variation of the fundamental constants [30, 31, 32, 33, 34, 35, 36]. Support for this hypothesis has emerged from recent observations of quasar absorption lines at redshift of  $z=1-2$  by Webb et al. [37, 38] that suggest the fine structure constant,  $\alpha$ , may have been smaller in the past (though see [39]). In some cases the variation of a fundamental constant is easily implemented in BBN because the nuclear physics aspects of the calculation are unaffected, but in others the lack of an adequate theory to predict such parameters as the nuclear binding energies and cross sections introduces a degree of uncertainty. An example is the calculation of Kneller & McLaughlin [36] who looked at the variation of  $\Lambda_{QCD}$ , its effects upon the binding energy of deuterons and the neutron-proton mass difference and, in turn, the impact upon BBN. In addition to variation of these nuclear parameters, variation of the constants relevant to nuclear structure might also partially stabilize nuclei that are presently particle unstable. For example, the lack of stable  $A = 5$  and  $A = 8$  nuclei is often cited as the explanation for the dearth of nuclei formed with masses above helium-4 though the endothermicity of pure strong reactions such as  ${}^4\text{He}(T, n){}^6\text{Li}$ ,  ${}^4\text{He}({}^4\text{He}, p){}^7\text{Li}$  and  ${}^4\text{He}({}^4\text{He}, n){}^7\text{Be}$  plays a role.

The focus in this paper is upon another nucleus that could also become stabilized - the dineutron  ${}^2\text{n}$ . The dineutron, a member of the nucleon-nucleon isospin triplet, is a spin singlet and, by itself, the dineutron is weakly unbound<sup>1</sup> by  $\sim 70$  keV, the n-n scattering length being negative [40, 41, 42, 43]. Early direct searches [44] did not see evidence for a stable dineutron but recently Bochkarev *et al.* [45] claim that  $45 \pm 10\%$  of the decay of an excited state of  ${}^6\text{He}$  is through the dineutron state<sup>2</sup> and Seth & Parker [47], amongst others, find evidence for dineutrons in  ${}^5\text{H}$ ,  ${}^6\text{H}$  and  ${}^8\text{He}$  decay. There is also a claim for tetraneutron,  ${}^4\text{n}$ , emission in the decay of  ${}^{14}\text{Be}$  [48].

Given that the dineutron is only weakly unbound, even small changes in the pion mass could, perhaps, result in a bound dineutron, although at present there is not enough experimental information to show whether or not this would occur [49, 50]. The scattering length is quite sensitive to the pion mass and so it is small changes in fundamental constants that change its mass, such as  $\alpha$ ,  $\Lambda_{QCD}$  or the Higgs vev, that could cause the dineutron to become bound. Since we are lacking an exact relationship between these fundamental constants and the binding energy of the dineutron we do not adopt a particular model for the time variation of fundamental constants, but instead explore the effect upon BBN of a bound dineutron directly.

In this paper we shall make an effort to derive a constraint upon the dineutron binding energy. We will consider the dineutron in isolation i.e. whatever the source of the new stability of the dineutron we shall limit the effect to just this nucleus. We begin with an overview of standard BBN in section §II with an emphasis on the details of the flow from free nucleons to helium-4 before proceeding to insert dineutrons in section §III. In section §IV we present our results for a baryon-to-photon ratio of  $\eta = 6.14 \times 10^{-10}$  and follow it up in §V with a discus-

---

\*Electronic address: Jim.Kneller@ncsu.edu

†Electronic address: Gail.McLaughlin@ncsu.edu

---

<sup>1</sup> Though it may become stable on the surface of neutron-rich nuclei.

<sup>2</sup> Bochkarev *et al.* [46] also have evidence of diproton emission from an excited state of  ${}^6\text{Be}$ .

sion of the errors in the calculation and any degeneracy with  $\eta$  in §VI. Finally, in §VII, we show how BBN can limit the dineutron binding energy before presenting our conclusions.

## II. BBN WITHOUT DINEUTRONS.

BBN can be simplistically broken into three phases characterized by the degree of equilibrium within the nucleons/nuclei.

During the first phase, at temperatures above  $T \gtrsim 1$  MeV, there are virtually no complex nuclei so that all the nucleons exist in a free state. The rapidity of the weak interactions in converting neutrons and protons,

$$n \leftrightarrow p + e + \bar{\nu}_e \quad (1a)$$

$$n + \bar{e} \leftrightarrow p + \bar{\nu}_e, \quad (1b)$$

$$n + \nu_e \leftrightarrow p + e, \quad (1c)$$

establish a weak equilibrium so that the neutron/proton ratio,  $F$ , is simply  $F \approx \exp(-\Delta_{np}/T)$ . As the Universe cools the rate at which neutrons must be converted to protons in order to maintain the equilibrium cannot be accommodated. As a consequence, the neutron-to-proton ratio departs from its equilibrium value and is said to ‘freeze-out’ even though conversion continues to occur. In the absence of neutron decay and the formation of complex nuclei, the ratio would attain an asymptotic value of  $F \sim 1/6$  [66, 67]. The departure of  $F$  from its equilibrium value denotes the boundary between the first two phases of BBN.

During the second phase of BBN, from a temperature of  $\sim 1$  MeV to  $\sim 100$  keV, the abundances of the various nuclei also begin to depart from equilibrium. At  $\sim 1$  MeV their abundances are suppressed relative to the free nucleons but the nuclear reactions that form them establish, and maintain, chemical/nuclear statistical equilibrium (NSE). In equilibrium the abundance<sup>3</sup>,  $Y_A = n_A/n_B$ , of a complex nuclei  $A$  is derived from  $\mu_A = Z\mu_p + (A - Z)\mu_n$  so after inserting the expressions for the Boltzmann number density we find

$$Y_A = \frac{g_A A^{3/2}}{2^A} \left[ n_B \left( \frac{2\pi}{m_N T} \right)^{3/2} \right]^{A-1} Y_p^Z Y_n^{A-Z} e^{B_A/T}. \quad (2)$$

Using  $F \sim 1/6$  and a baryon-photon ratio of  $\eta \sim 10^{-10}$  we see that for a temperature of  $T \sim 1$  MeV the abundance of deuterons is  $Y_D \sim 10^{-12}$ . After substituting  $Y_D$

for the thermal factors in equation (2) we obtain

$$Y_A = \frac{g_A A^{3/2}}{2 [3\sqrt{2}]^{A-1}} Y_p^{1+Z-A} Y_n^{1-Z} Y_D^{A-1} \times \exp\left(\frac{B_A - (A-1)B_D}{T}\right). \quad (3)$$

This equation now makes it much clearer that the abundance of a nucleus with mass  $A + 1$  is suppressed by approximately  $Y_D$  relative to the abundance of a nucleus with mass  $A$ .

If the neutron/proton abundances are held fixed then the NSE abundance has a minimum at  $T_A = 2B_A/(3A - 3)$ . Below  $T_A$  the various nuclear reactions provide sufficient nuclei to keep  $Y_A$  in equilibrium as the abundance climbs from the minimum but eventually a point is reached where this required production rate cannot be met and the abundance falls beneath the equilibrium value. This departure from equilibrium for the complex nuclei is in contrast with that of the neutrons where it was an insufficient rate that led to the departure, here it is a lack of reactants that is the cause. Heavier nuclei are the first to depart from equilibrium: helium-4 departs at  $T \sim 600$  keV while helium-3 and tritium drop out at  $T \sim 200$  keV. Below  $T \sim 200$  keV the only compound nucleus in NSE is the deuteron and its abundance controls the rate at which all the heavier nuclei can be produced. By  $T \sim 100$  keV the D abundance is approaching that of the free nucleons and the amount of D destruction, via such reactions as  $D(D, p)T$  and  $D(D, n)^3\text{He}$ , has become significant. When this occurs the deuteron abundance cannot be replenished sufficiently quickly to maintain its equilibrium and, consequently, it too departs from NSE. This final NSE departure forms the entrance to the third stage of BBN proper.

Below the deuteron NSE departure temperature the D abundance continues to grow for a short period but eventually the  $D + D$  drain tips the balance in favor of destruction and the deuteron abundance reaches a peak amplitude. The tritons and helions formed via the reactions  $D(D, p)T$  and  $D(D, n)^3\text{He}$  are produced in roughly equal amounts but the helions rapidly transform to tritium via  $^3\text{He}(n, p)T$ . The last step in the formation of the alpha particle is almost exclusively  $T(D, n)^4\text{He}$  which destroys  $\sim 1/3$  of all the deuterons formed. The essential steps in the scheme are illustrated in figure (1).

Smith, Kawano and Malaney [51] identified 8 reactions among the  $A \leq 4$  nuclei as being important for BBN. Five are identical to those in figure (1), the sixth is neutron-proton interconversion, and the two reactions they included, and which we have omitted from the figure, are  $^3\text{He}(D, p)^4\text{He}$  and  $T(p, \gamma)^4\text{He}$  both of which are 2 – 4 orders of magnitude smaller than  $T(D, n)^4\text{He}$ , so their importance is marginal. Whatever the exact number, this handful (or two) of important reactions is much smaller than the number of reactions included in any BBN code.

<sup>3</sup> The term ‘abundance’ is also used for the ratio  $Y_A/Y_H$

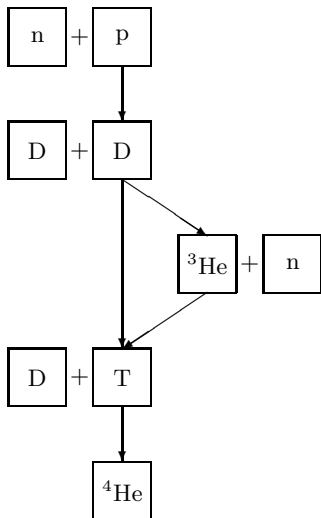


FIG. 1: A diagrammatic flow of nuclei in standard BBN. The complex nuclei are immersed in a (rapidly drained) bath of free nucleons and so we outline only where they form part of the set of reactants.

As the Universe cools eventually the Coulomb barriers in the various reactions become insurmountable leading to a cessation of the nucleosynthesis. The abundances have plateaued to their ‘primordial’ values with virtually every neutron now incorporated in helium-4 and only small residues in D, T and  $^3\text{He}$ . A small (but detectable) abundance of lithium-7 and beryllium-7 have also been formed but we will not discuss these two nuclei further.

### III. INSERTING DINEUTRONS INTO BBN

Inclusion of a new, light nucleus into BBN has the potential to significantly influence BBN and alter the predicted primordial abundances. These changes will occur because the dineutron will disrupt the flow of nucleons through the reaction network by both presenting new exit channels for reactions that already exist in BBN and through new entrance channels in the formation of the nuclei. One can construct a large number of plausible reactions in which dineutrons participate but not all are expected to play a prominent role for the same reason that standard BBN is dominated by only a few reactions. We can use our understanding of the important reactions in standard BBN to pick from the plethora of possibilities for dineutron reactions those which we expect to be important. The most important reactions involving dineutrons should be

- preferably exothermic,
- dominated by the strong interaction,
- and two-bodied in their entrance channel.

Exothermicity plays a pivotal role in the BBN because, during its second two phases, the system does not at-

tain an equilibrium and, typically, the flow of nuclei in any given reaction is one direction only. In a few cases where the Q-value for the reaction is less than few times the temperature during BBN (i.e.  $T \sim 100$  keV,  $Q \sim 500$  keV) flow may be in both directions because the ‘activation energy’ for an endothermic reaction is readily available. Examples of this behavior were seen in Kneller and McLaughlin [36]. The reaction should also be preferably strong in nature since this is the behavior seen in standard BBN where reactions such as  $\text{D}(\text{D}, \text{n})^3\text{He}$  dominate over  $\text{D}(\text{p}, \gamma)^3\text{He}$  though, in a few cases, such as  $\text{p}(\text{n}, \gamma)\text{D}$ , electromagnetic or weak interactions play an important role. The last requirement will remove those cases that pass the first two but whose entrance channels involve multiple particles.

From these requirements we have selected four dineutron reactions that we expect to be important:

$$\text{p} + {}^2\text{n} \leftrightarrow \text{D} + \text{n}, \quad Q = 2.22 \text{ MeV} - B_{2\text{n}}, \quad (4)$$

$$\text{D} + {}^2\text{n} \leftrightarrow \text{T} + \text{n}, \quad Q = 6.26 \text{ MeV} - B_{2\text{n}}, \quad (5)$$

$${}^3\text{He} + {}^2\text{n} \leftrightarrow {}^4\text{He} + \text{n}, \quad Q = 28.29 \text{ MeV} - B_{2\text{n}}, \quad (6a)$$

$${}^3\text{He} + {}^2\text{n} \leftrightarrow \text{T} + \text{D}, \quad Q = 2.99 \text{ MeV} - B_{2\text{n}}. \quad (6b)$$

The dineutron binding energy will determine the Q-value in these reactions and, if we permit values of  $B_{2\text{n}}$  of several MeV, both (4) and (6b) may reverse sign. We will not consider any changes to the other nuclear binding energies. Though one may expect a large change in the dineutron binding energy to be reflected in equally significant changes to the structure of the deuteron, the effects upon three nucleon nuclei may be considerably smaller [52]. In our study, we also do not consider reactions leading to the formation or destruction of nuclei above mass 4.

To this list we add three additional reactions:

$$\text{n} + \text{n} \leftrightarrow {}^2\text{n} + \gamma, \quad Q = B_{2\text{n}}, \quad (7)$$

$${}^2\text{n} \leftrightarrow \text{D}, \quad (8)$$

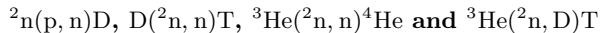
$${}^2\text{n} + \text{p} \leftrightarrow \text{T} + \gamma, \quad Q = 8.48 \text{ MeV} - B_{2\text{n}}. \quad (9)$$

These reactions could become important for producing and, more importantly, removing dineutrons. In particular, the inclusion of (8) and (9) is based on the following reasoning. Once we have dineutron cross sections we must integrate them over a Maxwell-Boltzmann spectrum to obtain a thermally averaged rate [53]. In all the dineutron reactions the lack of a Coulomb barrier means that the cross section for an exothermic reaction varies as  $1/\sqrt{E}$  at low energy and so the rate becomes a constant. This can have important consequences: written in terms of the temperature, a reaction such as  $A + B \rightarrow X$ , with a rate per particle pair  $\Gamma$ , destroys nucleus  $A$  at a rate

$$\frac{dY_A}{dT} \propto \Gamma Y_A Y_B \quad (10)$$

where we have used the relations  $n_B \propto T^3$  and  $T^2 \propto 1/t$ . If we assume the abundance of nucleus  $B$  is much larger than  $A$ 's and does not change by any other process then the solution to this equation is  $Y_A \propto \exp(\Gamma Y_{B0} T)$  where  $Y_{B0}$  is the abundance of  $B$  at some fiducial temperature. In this scenario, the abundance of  $A$  never becomes a constant and BBN would never end! In standard BBN this situation never arises because the two temperature-independent reactions,  $p(n, \gamma)D$  and  ${}^3\text{He}(n, p)T$ , are killed by the decay of the neutron. But if the dineutron becomes stable then without a reaction such as  ${}^2n(p, \gamma)T$  the dineutron abundance could plateau to a constant larger than, say, the abundance of helium-3 and the circumstances of equation (10) may be realized in the reaction  ${}^3\text{He}({}^2n, n){}^4\text{He}$ . In order to obtain a primordial abundance of  ${}^3\text{He}$  it is imperative that this situation be prevented. The decay of the dineutron and  ${}^2n(p, \gamma)T$  will ensure this by depleting the final dineutron abundance for all values of  $B_{2n}$  we shall explore.

Now that we have determined the most important reactions, we need cross sections for them before we can proceed.



Since the dineutron is presently unstable we posit cross sections based on ‘similar’ strong reactions involving deuterium or other light nuclei. If we consider an arbitrary two-body strong reaction  $i+j \leftrightarrow k+l$  then general considerations lead us to expect a cross section per particle pair which is proportional to a matrix element squared, the phase space with an energy conserving delta function and inversely proportional to a flux. In nuclear astrophysics, one typically writes the cross section as

$$\sigma(E) = \frac{S(E)}{E} \exp\left(-\pi \alpha Z_i Z_j \sqrt{\frac{2\mu_{ij}}{E}}\right) \quad (11)$$

where  $\mu_{ij}$  is the reduced mass for incoming particles  $i$  and  $j$ , and  $S(E)$  is the astrophysical S-factor. For our purposes, this parameterization is not sufficient since it does not explicitly show the effects of a Q value upon the final states. This is particularly crucial since in our study Q-values will vary as the dineutron binding energy varies. With that in mind, we write the non-resonant (S-wave) contributions to the cross section, following [54, 55], as proportional to the product of both Coulomb penetrability factors  $G_{ij}(E)$  and  $G_{kl}(E+Q)$ , the available phase space in the exit channel  $\Phi_{kl}(E+Q)$  together with the statistical weight  $g_{kl}$  and the reciprocal of the entrance channel velocity. The penetrability factor for charged particle interactions,  $G_{ij}(E)$ , is simply

$$G_{ij}(E) = \sqrt{\frac{E_{ij}^C}{E}} \exp\left(-\pi \alpha Z_i Z_j \sqrt{\frac{2\mu_{ij}}{E}}\right) \quad (12)$$

where  $E_{ij}^C$  is the Coulomb barrier energy [56]. Although in the standard cross section parameterization, shown

in equation (11), the second Coulomb penetrability factor can be absorbed into the astrophysical S factor because, typically, the energy is much smaller than the Q-value, here we retain it explicitly. The phase space factor,  $\Phi_{kl}(E+Q)$ , is

$$\Phi_{kl}(E+Q) \propto \sqrt{(E+Q)\mu_{kl}^3} \quad (13)$$

while the statistical weight factor  $g_{kl}$  accounts for the multiplicity of the final state

$$g_{kl} = (2J_k + 1)(2J_l + 1) \quad (14)$$

where  $J_k$  and  $J_l$  are the spins of the individual nuclei. The reciprocal of the entrance channel velocity is proportional to  $\Phi_{ij}/(\mu_{ij}E)$ . Putting all these together the cross section for the reactions  $i+j \leftrightarrow k+l$  is expected to be of the form

$$\begin{aligned} \sigma_{i+j \rightarrow k+l}(E) &= S_{ij,kl}(E) \frac{g_{kl}}{\mu_{ij}E} G_{ij}(E) G_{kl}(E+Q) \\ &\times \Phi_{ij}(E) \Phi_{kl}(E+Q). \end{aligned} \quad (15)$$

where we have introduced  $S_{ij,kl}(E)$  as an undetermined function. This function becomes constant at low energy, and is similar to, but not the same as, the astrophysical S-factor.

With the help of equation (15) we can extract the most obvious behavior of any cross section with energy to derive  $S_{ij,kl}(E)$ . Our expectation is that this quantity varies slowly though of course the exact details of a reaction may lead to significant departures. After extracting  $S_{ij,kl}(E)$  from some known reaction we can then insert it into the similar dineutron reaction based on the assumption that  $S_{ij,kl}$  does not change considerably from one to the other. The major changes in the cross sections will therefore be limited to the considerable effects of the Coulomb barrier penetrability and phase space. We have examined the validity of this approach by using it to predict  $D(D, p)T$  from  $D(D, n){}^3\text{He}$ , and  $T(D, n){}^4\text{He}$  from  ${}^3\text{He}(D, p){}^4\text{He}$ . The last two cross section are dominated by large resonances corresponding to excited states of  ${}^5\text{He}$  and  ${}^5\text{Li}$  [59] but the non-resonant pieces have been extracted by Chulick *et al.* [57] allowing us to compare the transformation. In both test cases we find the transformation works reasonably well with an error that is a factor of order a few.

For the  ${}^2n(p, n)D$  reaction there is no similar deuteron reaction with which to compare so instead we used the broadly similar  ${}^3\text{He}(n, p)T$ . We have been unable to find an analytic expression for this cross section so we interpolated the ENDF-IV evaluated cross section data available online [58] and then factored out the expected behavior shown in equation (15) before replacing it with the appropriate terms for  ${}^2n+p \leftrightarrow D+n$ .

We expect the  $D+{}^2n \leftrightarrow T+n$  cross section to be similar to  $D(D, p)T$  and  $D(D, n){}^3\text{He}$  up to corrections for the Coulomb barrier penetrability and phase space factors. Here we have analytic expressions of the S-factor to use from Chulick *et al.* [57].

To estimate the last two reactions,  ${}^3\text{He} + {}^2\text{n} \leftrightarrow \text{n} + {}^4\text{He}$  and  ${}^3\text{He} + {}^2\text{n} \leftrightarrow \text{D} + \text{T}$ , one appeals to their similarity with  $\text{T}(\text{D}, \text{n}){}^4\text{He}$  so that one may use the Chulick *et al.* [57] expression and, once again, correct for the change in the phase space, Coulomb barrier penetrability etc. As mentioned earlier, the  $\text{T}(\text{D}, \text{n}){}^4\text{He}$  cross section exhibits a resonance due to an excited state of the  ${}^5\text{He}$  nucleus (see [59] for an energy level diagram). The position of this same resonance, relative to the  ${}^3\text{He} + {}^2\text{n}$  ground state, depends on the dineutron binding energy being subthreshold for  $B_{2\text{n}} \lesssim 3$  MeV. In addition, there are further excited states of  ${}^5\text{He}$  that become relevant when  $B_{2\text{n}} \sim 0$  but, as we will show, the effects of the dineutron become apparent only when  $B_{2\text{n}}$  approaches  $B_{\text{D}}$  and we have not added them to our cross section.



This weak reaction is actually the sum of *four* sub-processes:

$${}^2\text{n} \leftrightarrow \text{D} + e + \bar{\nu}_e \quad 0 \leq E_\nu \leq \Delta_{2\text{nD}} - m_e \quad (16\text{a})$$

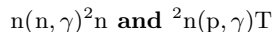
$${}^2\text{n} + \nu_e \leftrightarrow \text{D} + e \quad -\Delta_{2\text{nD}} + m_e \leq E_\nu \quad (16\text{b})$$

$${}^2\text{n} + \bar{e} \leftrightarrow \text{D} + \bar{\nu}_e, \quad \Delta_{2\text{nD}} + m_e \leq E_\nu \quad (16\text{c})$$

$${}^2\text{n} + \bar{e} + \nu_e \leftrightarrow \text{D} \quad 0 \leq E_\nu \leq -\Delta_{2\text{nD}} - m_e \quad (16\text{d})$$

where we have denoted by  $\Delta_{2\text{nD}}$  the dineutron-deuteron mass difference i.e  $\Delta_{2\text{nD}} = \Delta_{\text{nD}} + B_{\text{D}} - B_{2\text{n}} = 3.52$  MeV  $- B_{2\text{n}}$ . We do not consider those cases where the final states are free nucleons. From the limits on the neutrino energy,  $E_\nu$ , we see that, at most, only three of these reactions can be operant at any given value of  $B_{2\text{n}}$ . For these rates we use expressions similar to the neutron-proton interconversion rates but with different Q-values and a matrix element that takes into account the presence of two neutrons. We also use a pure Gamow-Teller decay between the  $0^+$  ground state of the dineutron and the  $1^+$  ground state of the deuteron. While there remains some uncertainty in the rates it has a much smaller impact on final abundance yields as compared with the uncertainties in the strong interaction rates discussed above.

There is one interesting quirk that appears when  $\Delta_{2\text{nD}} < m_e$ , which is that an atom of deuterium can capture an electron to form a dineutron. Although interesting this process has not been included in our calculations because the amount of atomic deuterium is negligible at the temperatures relevant to BBN. We also see that spontaneous deuteron decay can occur when  $\Delta_{2\text{nD}} < -m_e$  i.e. when  $B_{2\text{n}} \gtrsim 4$  MeV. Though this possibility remains interesting we shall not pursue dineutron binding energies that permit this reaction to occur.



Though  $\text{n}(\text{n}, \gamma){}^2\text{n}$  looks similar to deuteron formation via  $\text{n}(\text{p}, \gamma)\text{D}$  this reaction is suppressed because there is

no charge. Despite this smallness, it is the only exothermic reaction capable of producing dineutrons when  $B_{2\text{n}}$  is small. Following Rupak [60], the lowest order contribution to this cross section should be something like  $(N^T \sigma_2 \otimes \tau_2 \tau_j N)^\dagger (N^T \sigma_2 \otimes \tau_2 \tau_j (\vec{D}_k + \vec{D}_k) N) E_k$  and  $(N^T \sigma_2 \otimes \tau_2 \tau_j N)^\dagger (N^T \sigma_2 \sigma_i \otimes \tau_2 \tau_j (\vec{D}_k - \vec{D}_k) N) B_l \epsilon^{ikl}$ . From examining the  $\text{n}(\text{p}, \gamma)\text{D}$  operators in the cross section from Rupak we estimated that this lowest order contribution is  $\text{N}^4\text{LO}$ . We therefore make an order of magnitude estimate for the dineutron cross section by starting with the  $\text{n}(\text{p}, \gamma)\text{D}$  (which has a leading order contribution) and suppressing it by the appropriate factor. Although there is considerable error, just as with the two  ${}^3\text{He} + {}^2\text{n}$  reactions, the effects of the dineutron will only become apparent when  $B_{2\text{n}}$  approaches  $B_{\text{D}}$  by which time this reaction will be of little importance.

The  ${}^2\text{n}(\text{p}, \gamma)\text{T}$  reaction has been included as a failsafe mechanism to remove dineutrons since it is exothermic for all  $B_{2\text{n}}$ . It is not expected to be an important reaction unless we strongly deviate from the nucleon flow in standard BBN because the similar, standard BBN reaction  $\text{D}(\text{n}, \gamma)\text{T}$  is also unimportant. We have also estimated its cross section from the  $\text{n}(\text{p}, \gamma)\text{D}$  reaction in [60] after modifying the phase space and spin multiplicity factors using the expressions discussed above.

#### IV. THE EFFECTS OF A BOUND DINEUTRON UPON BBN.

The chief manner in which the dineutron affects BBN is via the Q-values for the reactions and, from the values quoted earlier, we can identify three regions of  $B_{2\text{n}}$  up to the 4 MeV limit we considered. They are:

- $B_{2\text{n}} \leq B_{\text{D}}$ ,
- $B_{\text{D}} \leq B_{2\text{n}} \leq 3.0$  MeV, and
- $3.0$  MeV  $\leq B_{2\text{n}}$ .

In figure (2) we plot the fractional change in the primordial abundance relative to standard BBN at  $\eta = 6.14 \times 10^{-10}$  and the three regions we have identified are clearly visible. Up to  $B_{\text{D}}$  there is no discernable change with  $B_{2\text{n}}$ , over the interval  $B_{\text{D}} \leq B_{2\text{n}} \leq 3.0$  MeV the deuterium and helium-3 abundances drop and the helium-4 abundance rises but after 3.0 MeV the helium-3 and helium-4 abundances plateau and the evolution of  $Y_{\text{D}}$  changes noticeably. In what follows we shall explain why and how the dineutron influences BBN in each region.

##### A. $B_{2\text{n}} \leq B_{\text{D}}$

For  $B_{2\text{n}} \ll B_{\text{D}}$  the dineutron lifetime is of order 1 s so while the decay would appear to be a significant drain on the dineutron abundance any loss is easily, and rapidly,

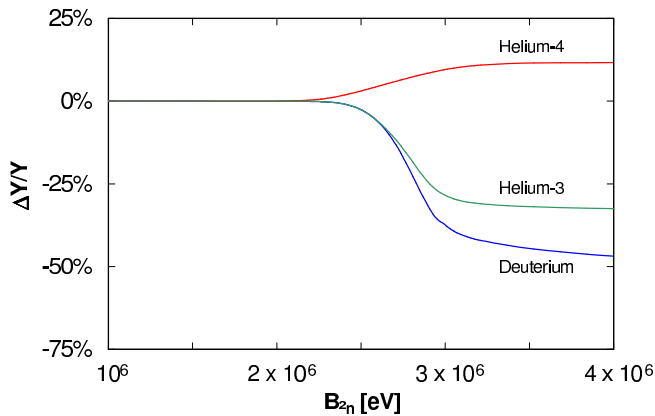


FIG. 2: The fractional change in the primordial deuterium, helium-3 and helium-4 abundances as a function of the dineutron binding energy.

replaced from the pool of free neutrons and, consequently, the dineutron abundance during the second stage of BBN follows its NSE value:

$$Y_{2n} = \frac{1}{3} \frac{Y_n Y_D}{Y_p} \exp\left(\frac{B_{2n} - B_D}{T}\right). \quad (17)$$

Therefore the effect of increasing the dineutron binding energy is the same as one expects from NSE, i.e. the abundance builds up at higher temperature as the binding energy increases. The evolution of the dineutron abundance as a function of the temperature for the four cases  $B_{2n} \in \{10^4 \text{ eV}, 10^6 \text{ eV}, 2 \times 10^6 \text{ eV}, B_D\}$  is shown in figure (3). In every example in the figure the dineutron abundance is smaller than the deuteron abundance: even when  $B_{2n} = B_D$  the NSE abundance is smaller than  $Y_D$  due to both the smaller abundance of free neutrons ( $Y_n/Y_p \sim 1/6 - 1/7$ ) and the spin factor,  $1/3$ , of

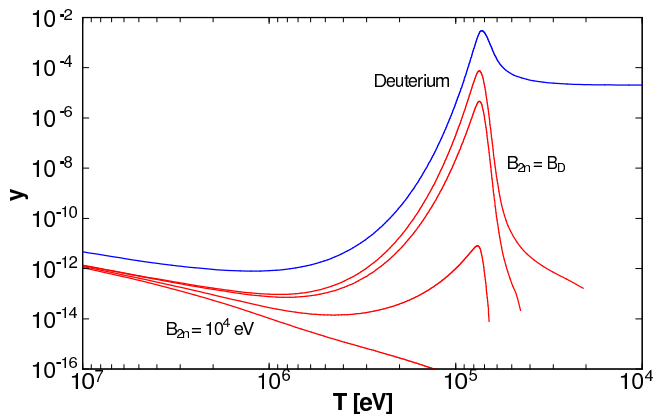


FIG. 3: The evolution of the dineutron abundance as a function of the temperature for  $B_{2n} \in \{10^4 \text{ eV}, 10^6 \text{ eV}, 2 \times 10^6 \text{ eV}, B_D\}$  and the deuteron abundance from standard BBN.

deuterons, combining for a total of  $\sim 1/20$ . The figure also makes it quite clear that as  $B_{2n}$  approaches  $B_D$  the dineutron starts to possess a considerable abundance at the transition to BBN proper, approximately the location of the deuteron peak. And the figure also shows that the position of the peak dineutron abundance is unaffected by its binding energy and is coincident with the deuteron peak. Whatever the dineutron binding energy in this range BBN proper is still initiated by the deuteron's departure from NSE and the small amount of dineutrons present at that time is rapidly removed. When  $B_{2n} \ll B_D$  their small abundance means that they never form a substantial population which could possibly influence the predictions of BBN but as  $B_{2n}$  approaches  $B_D$  their presence at  $T_{BBN}$  becomes important.

### B. $B_D \leq B_{2n} \leq 3.0 \text{ MeV}$

As shown above, the NSE dineutron abundance at  $T \sim 100 \text{ keV}$  when  $B_{2n} = B_D$  is smaller than  $Y_D$  by roughly a factor of  $1/20$  so it is not until the dineutron binding energy has grown to the point where it is capable of reversing the suppression of its NSE abundance by the neutron-to-proton ratio and the spin of the deuteron that its abundance approaches  $Y_D$  at  $T \sim 100 \text{ keV}$ . Roughly this occurs when

$$\exp\left(\frac{B_{2n} - B_D}{T}\right) \sim 20 \quad (18)$$

i.e. when  $B_{2n} \sim 2.5 \text{ MeV}$ . The evolution of the dineutron and deuteron abundances during this interval for  $B_{2n}$  is shown in figure (4) and confirms that the dineutron abundance surpasses the deuteron abundance at  $B_{2n} \sim 2.5 \text{ MeV}$ . The figure also demonstrates a number of new features: the position of the dineutron peak abundance now moves to higher temperatures as  $B_{2n}$  increases, the peak deuteron abundance drops and the temperature at which it departs NSE also shifts to higher temperatures. These effects ripple through to the triton and helion as shown in figure (5). As  $B_{2n}$  increases tritium and helium-3 depart NSE at lower temperatures: the change isn't dramatic, by  $B_{2n} = 3 \text{ MeV}$  the two  $A = 3$  nuclei depart at  $T \sim 170 \text{ keV}$  rather than at around  $200 \text{ keV}$  in standard BBN but the sensitivity of the NSE abundance to the temperature means that the abundance of helium-3 and tritium after this point is roughly  $2 - 3$  orders of magnitude larger. The figure also shows that the movement of the tritium peak parallels that for dineutrons by shifting to higher temperatures as  $B_{2n}$  increases.

The movements in the abundances of the intermediary nuclei are all attributable to changes in the flow of the nuclei through the reaction network. For  $B_{2n} \geq B_D$ , the reaction  $D(n, p)^2n$  is now exothermic and a detailed examination of the nuclear flow at  $B_{2n} = 2.6 \text{ MeV}$  confirms this to be the source of dineutrons. The flow also indicates the dineutrons are then chiefly converted to tritons via

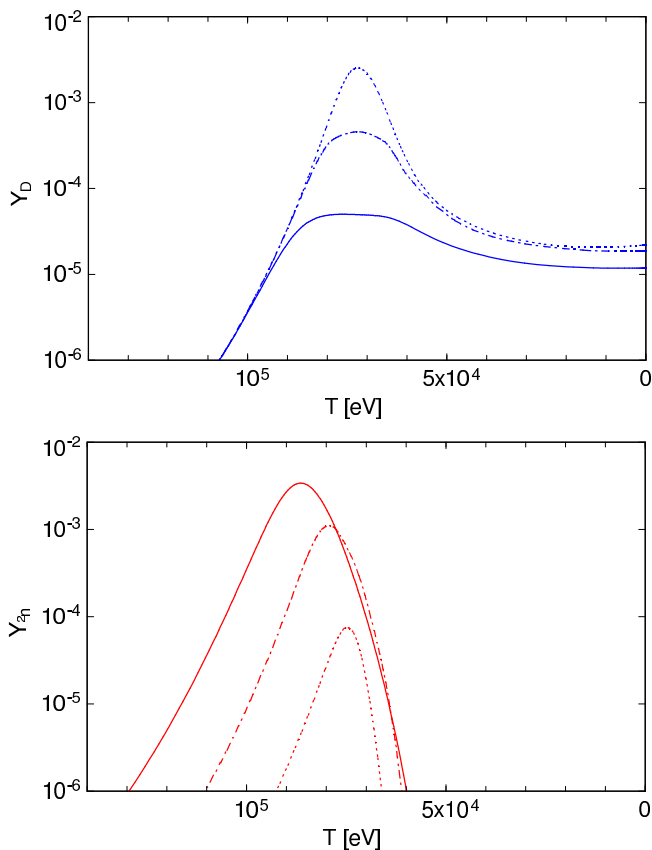


FIG. 4: The evolution of the deuterium (top panel) and dineutron (bottom panel) abundances as a function of the temperature for  $B_{2n} \in \{B_D$  (dotted line), 2.6 MeV (dot-dashed line), 3 MeV (solid line) $\}$ .

the reaction  ${}^2n(D, n)T$ . Both reactions lead to a disruption of the usual mechanisms that lead to BBN proper. In standard BBN the transition to BBN proper was due to the removal of deuterons via the two  $D + D$  processes but now, because beyond  $B_{2n} \sim 2.5$  MeV the NSE abundance of dineutrons is *larger* than that of deuterons and because free neutrons are so plentiful during the second stage of BBN, the departure occurs earlier. Remarkably both  $D(D, n){}^3\text{He}$  and  $D(D, p)T$  are now of little consequence. The shift in the deuterons' NSE departure temperature is not large, figure (4) demonstrates this, but, as with  $T$  and  ${}^3\text{He}$ , the deuterons' NSE abundance is very sensitive to the temperature. The  ${}^2n(D, n)T$  reaction can also provide sufficient tritium to keep its abundance in equilibrium until a slightly lower temperature. The switch in the mechanism that initiates BBN proper explains many of the features seen in figures (4) and (5).

From the nuclear flow we also find that helium-3 no longer plays an important role in the formation of helium-4. Some helium-3 is still formed, via  $D(D, n){}^3\text{He}$ , but this source is suppressed due to the lack of deuterons; what little helium-3 is created is processed to tritium by the usual  ${}^3\text{He}(n, p)T$  though  ${}^2\text{He}({}^2n, n){}^4\text{He}$  does play a role.

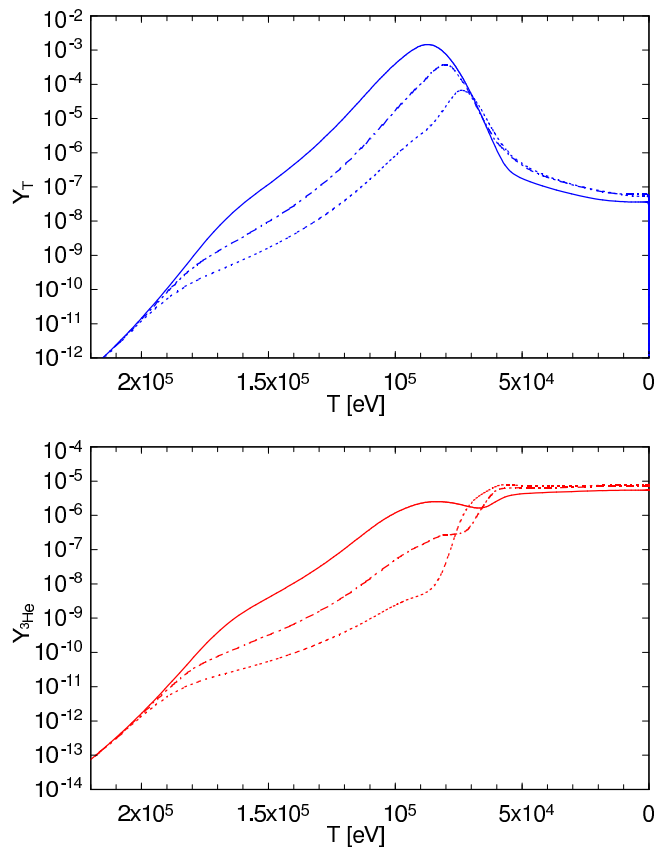


FIG. 5: The evolution of the tritium (top panel) and helium-3 (bottom panel) abundances as a function of the temperature for  $B_{2n} \in \{B_D$  (dotted line), 2.6 MeV (dot-dashed line), 3 MeV (solid line) $\}$ .

The reduced significance of helium-3 is not reflected in figure (5): one must remember that the net rate of formation for the intermediary  $D$ ,  $T$  and  ${}^3\text{He}$  is the small difference between production and destruction and does not necessarily indicate the true amount of nucleons flowing through them. Even in standard BBN the evolution of helium-3 does not resemble that of tritium because  ${}^3\text{He}(n, p)T$  is so rapid and one can only see the significance of the helium-3 nucleus by examining the individual reaction rates [51].

Finally, the formation of helium-4 still occurs via  $T(D, n){}^4\text{He}$  and, due to the earlier initiation of BBN proper, its final (primordial) abundance is enhanced. The reaction network is modified and the bulk of the nucleons now flow through a network resembling that shown in figure (6).

By  $B_{2n} = 3$  MeV figure (4) shows that the peak abundance of deuterons has dropped by two orders of magnitude from that in standard BBN and BBN proper begins at an even higher temperature. The nuclear flow now indicates that tritium formation is increasingly dominated

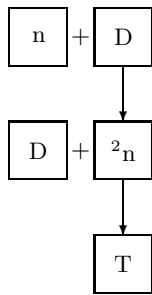


FIG. 6: The schematic flow of nuclei through the reaction network from deuterium to tritium at  $B_{2n} = 2.6$  MeV. The flow does not include helium-3. A little of this nucleus is still produced via  $D(D, n)^3\text{He}$  but the suppressed deuteron abundance means that the amount is substantially reduced compared to standard BBN.

by  ${}^2\text{n}(p, \gamma)\text{T}$  rather than  ${}^2\text{n}(D, n)\text{T}$  and, interestingly, the dominant source of helium-3 is the mildly endothermic  $\text{T}(p, n)^3\text{He}$  at higher temperatures with a changeover to  $\text{T}(D, {}^2\text{n})^3\text{He}$  as the Universe cools. This flow,  $\text{T}(p, n)^3\text{He}$ , is opposite to that in standard BBN,  ${}^3\text{He}(n, p)\text{T}$ .

This second region of  $B_{2n}$  is where the presence of dineutrons really becomes manifest. At  $B_{2n} = B_D$  the dineutron is just starting to influence BBN, by  $B_{2n} = 3$  MeV it has considerably altered the reaction network that take the free neutrons to helium-4 and led to a significant change in the mechanism that leads to BBN proper.

### C. $3.0 \text{ MeV} \leq B_{2n}$

The excitement seen when  $B_D \leq B_{2n} \leq 3$  MeV has largely played out as we enter the third domain of  $3 \text{ MeV} \leq B_{2n}$  and the shifts in the evolution of the abundances slows. In this range, between 3 MeV and 4 MeV, there are no, new, major changes in the nuclear flow because the Q-values of the most important reactions are now all  $\sim$  MeV. Nevertheless, a detailed study of the reaction network does show small differences and we discuss those here.

Although further increases in the dineutron binding energy are not reflected in the position and amplitude of the peak dineutron abundance, the temperature at which the dineutron departs NSE shifts to higher values with  $B_{2n}$ . In contrast, the reduction in the amplitude of the peak deuteron abundance seen in figure (4) becomes less dramatic and its NSE departure temperature has all but ceased to move as  $B_{2n}$  increases.

The behavior of the evolution of these two  $A = 2$  nuclei reflect the fact that dineutrons are primarily created from deuterons and that the dominant dineutron destruction mechanism has switched from  ${}^2\text{n}(D, n)\text{T}$  to  ${}^2\text{n}(p, \gamma)\text{T}$ . Dineutron NSE departure occurs because of insufficient production from the small D abundance. The  ${}^2\text{n}$  abundance at lower temperatures is thus controlled by the deuteron. The reaction  ${}^2\text{n}(p, \gamma)\text{T}$  is affected by  $B_{2n}$

only through the exit channel phase space which varies as  $\sqrt{B_T - B_{2n}}$ . With an abundance controlled by D and a destruction mechanism that varies only weakly with  $B_{2n}$  the height and temperature of the peak dineutron abundance is, essentially, static. Deuteron departure from NSE occurs when its abundance opens the  $D(n, p){}^2\text{n}$  drain and, again,  $B_{2n}$  only enters weakly through the exit channel phase space.

A new feature emerges in this third region of  $B_{2n}$ . At  $B_{2n} \geq 3.0$  MeV, the Q-value for the reaction  ${}^3\text{He}({}^2\text{n}, D)\text{T}$  is now negative and the importance of the helion as an intermediary in the formation of helium-4 rebounds, though not to the level in standard BBN. The source of helions is principally the mildly endothermic  $\text{T}(p, n)^3\text{He}$  but switches to  $\text{T}(D, {}^2\text{n})^3\text{He}$  as the Universe cools.

Finally, helium-4 is now chiefly formed by both  $\text{T}(D, n){}^4\text{He}$  and  $\text{T}(\text{T}, 2n){}^4\text{He}$  in almost equal proportions with minor contributions from  $\text{T}(p, \gamma){}^4\text{He}$  and  ${}^3\text{He}({}^2\text{n}, n){}^4\text{He}$ . The network has changed slightly and the new flow at  $B_{2n} = 3.5$  MeV is illustrated in figure (7).

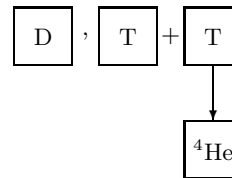


FIG. 7: The diagrammatic flow of nuclei through the reaction network from tritium onwards at  $B_{2n} = 3.5$  MeV.

## V. ARE THESE PREDICTIONS ROBUST?

While we have strived to estimate the various dineutron cross sections by basing them upon simple physical assumptions, it is a worthwhile task to see how robust the effects we have described are. If we know (or assume) the distribution for the error, either in the cross-section or the thermally averaged rate, then one can compute the error matrix as in Fiorentini *et al.* [62] and Cuoco *et al.* [61] though this approach cannot recover higher moments of the abundance distribution. An alternative is to construct the distribution of the abundances by sampling the distribution of the errors in a Monte Carlo analysis. This technique was used by Krauss & Romanelli [63], Smith, Kawano & Malaney [51], Krauss & Kernan [64] and, more recently, Nollett and Burles [65] and is the technique we shall use. To this end we introduced random multiplicative factors for all our dineutron reaction cross sections with the exception of  ${}^2\text{n} \leftrightarrow D$ , the most reliably estimated. These factors were chosen from a probability distribution limited to the range between  $1/5$  and  $5$  and weighted such that there was equal probability either side of  $1$ . The baryon-to-photon ratio was



fixed at  $\eta = 6.14 \times 10^{-10}$ . In figure (8) we plot the root

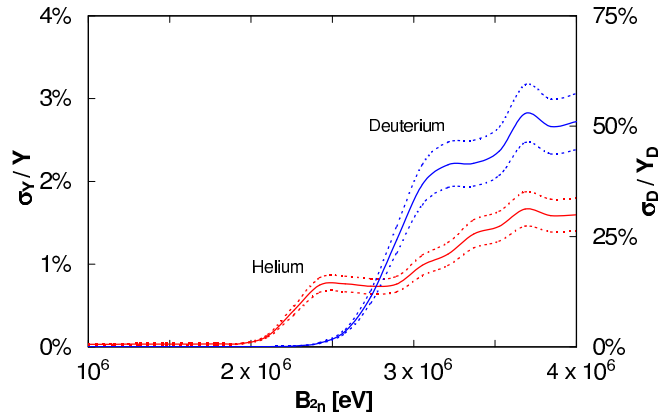


FIG. 8: The root mean square deviation divided by the mean plus the  $\pm 3\sigma$  error for deuterium and helium-4 as a function of the dineutron binding energy. Below  $B_{2n} \sim 2$  MeV neither nucleus exhibits any spread due to the uncertainty in the dineutron reaction rates. Above this value the spread in the deuterium results becomes large while the results for helium remain smaller than  $\sim 2\%$  for all value of  $B_{2n}$ .

mean square deviations for deuterium and helium-4 and the three regimes for the dineutron binding energy are clearly visible in both curves. The increasing spread for both reflects the increasing dominance of dineutron reactions in the formation of helium-4. The figure shows that up to  $B_{2n} \sim 2$  MeV the errors in the reactions involving dineutrons do not introduce any error into the predicted abundances, illustrating again the insignificance of dineutrons in BBN when their binding energy is smaller than this value. Above  $B_{2n} \sim 2$  MeV the curves begin to deviate from zero but note two important features: first, the spread in helium-4 is small for all values of  $B_{2n}$ , and second, the spread in the predicted abundance of deuterium does not exceed  $\pm 100\%$ . The small spread in the helium-4 curves indicate that we can reliably predict the abundance of helium-4 even if dineutrons have significantly impacted BBN, while the fact that the deuterium curves do not exceed 100% shows that at least the *direction* of the change is known even if the exact abundance is not. We have not shown the rms spread for helium-3 because it exceeded  $\pm 100\%$ .

Note also that the range in the abundances is significantly smaller than the range we permitted for the random factors. This may seem remarkable since the primordial abundance of an intermediary nuclei, such as deuterium, involves a fierce competition between its production and destruction and hence the adopted cross sections. While dineutrons may have led to significant departures in the flow of nuclei compared to standard BBN, large variations in the dineutron reaction rates do not translate into equally large spreads in the abundances of the intermediaries.

We also found that there was a significant anti-correlations in the results as shown in figure (9). For

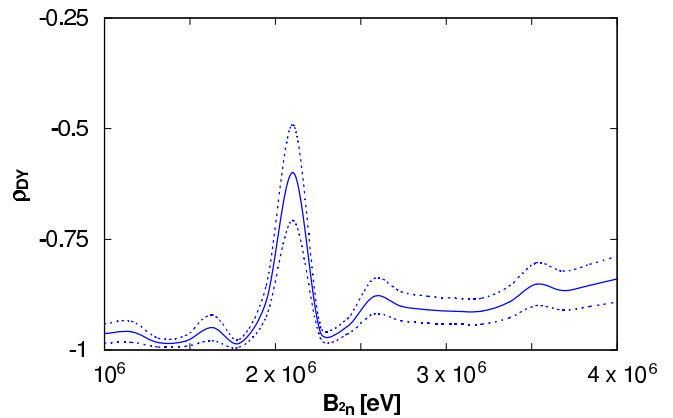


FIG. 9: The correlation between the deuterium abundance and helium-4 mass fraction,  $\rho_{DY}$ , and its  $\pm 3\sigma$  error, as a function of the dineutron binding energy. Below  $B_{2n} \sim 2$  MeV the correlation is close to  $-100\%$  while after  $B_{2n} \sim 3$  MeV the correlation has softened to  $\sim -80\%$ . The large peak at  $B_{2n} \sim 2$  MeV corresponds to the point where the change in the flow of nuclei through the reaction network occurs.

$B_{2n} \lesssim 2$  MeV the correlation coefficient was almost exactly  $-1$  while over the interval  $2.5 \text{ MeV} \lesssim B_{2n} \lesssim 3 \text{ MeV}$  the anti-correlation softened slightly to  $\sim -0.8$ . As a consequence of this correlation the covariance matrix,  $V_R$ , describing the error in the predictions arising from the uncertainties in the dineutron's reaction rates, contains off-diagonal pieces.

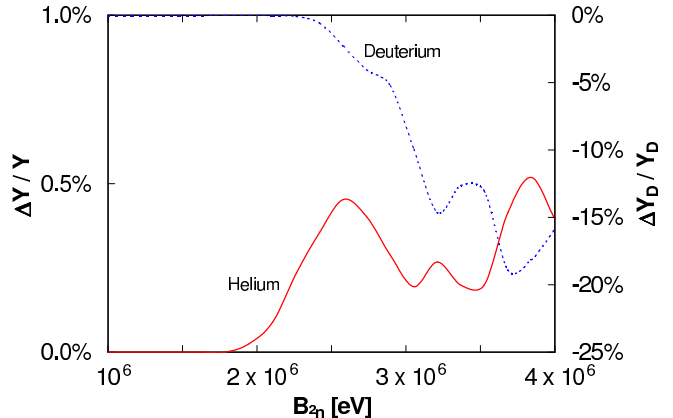


FIG. 10: The fractional difference between the mean from the Monte Carlo simulation and the result with no random factors. The solid line is for helium-4, the dotted is for deuterium.

We have delayed until last the difference we find in the mean from the sample and the primordial abundances we derive with no random factors as shown in figure (2). The fact that a discrepancy arises is not surprising given the non-linearity of BBN. The errors (which are functions of  $B_{2n}$ ) for helium-4 is  $\lesssim 0.5\%$  but for deuterium it reaches  $\lesssim 20\%$  and helium-3 fared even worse with a discrepancy

between the mean and no random factors approaching 30%. The fractional difference between the mean and the result with no random factors are shown in figure (10) for deuterium and helium-4. Although seemingly large, this error is smaller than the statistical fluctuations for all three nuclei (seen in figure (8) for deuterium and helium-4) but not significantly so and we must include it in the total error for the predictions as a systematic. The covariance matrix for the systematic error is denoted by  $V_S$ .

With means,  $\bar{\mathbf{Y}}$ , and variance,  $V_T = V_R + V_S$ , that are functions of  $B_{2_n}$  we approximate the distributions in the predictions as Gaussians

$$P(\mathbf{Y}|B_{2_n}) = \frac{1}{\sqrt{2\pi|V_T|}} \times \exp\left[-\frac{1}{2}(\mathbf{Y} - \bar{\mathbf{Y}})^T V_T^{-1} (\mathbf{Y} - \bar{\mathbf{Y}})\right]. \quad (19)$$

We have checked the validity of this approximation to the spread in the results by performing a Kolmogorov test at each value of  $B_{2_n}$  we set. The spread in the predictions for helium-3, which we have not shown, did not pass this due to a significant kurtosis.

## VI. A DEGENERACY WITH $\eta$ ?

So far we have restricted our discussions to a fixed value of the baryon-to-photon ratio,  $\eta$ , but if we allow this parameter to also vary we may well end up with a degeneracy that makes it difficult to establish the presence of a bound dineutron. To determine if this occurs,

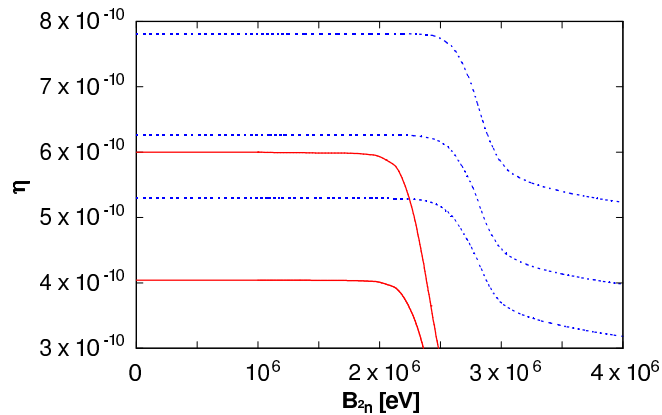


FIG. 11: Helium-4 iso-mass fraction (solid) and Deuterium iso-abundance (dashed) contours in the  $B_{2_n} - \eta$  plane. From top to bottom, the helium-4 contours are  $Y = 0.248$  and  $Y = 0.244$  and the deuterium abundances are  $D/H = 1.8 \times 10^{-5}$ ,  $D/H = 2.6 \times 10^{-5}$  and  $D/H = 3.4 \times 10^{-5}$ .

we show in figure (11) iso-abundance and iso-mass fraction contours for deuterium and helium respectively as a function of  $B_{2_n}$  and  $\eta$ . If we examine the most robust prediction of our modified BBN, the increase in  $Y$ , then we

can quite easily mask this effect by *lowering*  $\eta$  as shown in the figure. The decrease in  $\eta$  required to offset the increase in the primordial mass fraction as  $B_{2_n}$  increases is considerable so that above  $B_{2_n} \sim 2.5$  MeV all values of  $\eta$  in the  $3 \times 10^{-10}$  to  $8 \times 10^{-10}$  range plotted yield a helium-4 mass fraction above 0.248. For deuterium, lower values of  $\eta$  lead to increases in the final abundance so that they too can mitigate the decrease in  $Y_D$  as  $B_{2_n}$  increases. But the figure shows that the decrease in  $\eta$  required for deuterium is nowhere near as large as that required for helium-4, so, while there is an anticorrelation of  $B_{2_n}$  and  $\eta$  for both helium-4 and deuterium, there is no degeneracy for both simultaneously. If we considered each species separately then the degeneracy could, instead, be broken by using the CMB since lowering  $\eta_{BBN}$  will lead to a discrepancy with  $\eta_{CMB}$ .

## VII. AN UPPER LIMIT FOR $B_{2_n}$

It's finally time to derive an upper limit to  $B_{2_n}$  based on the compatibility with observations. The primordial abundance, D/H, of deuterium is taken to be  $D/H = (2.6 \pm 0.4) \times 10^{-5}$  [14] while we will consider both the Olive, Steigman and Walker [68] value of  $Y_{OSW} = 0.238 \pm 0.005$  and the Izotov and Thuan value of  $Y_{IT} = 0.244 \pm 0.002$  [69, 70] for the helium-4 mass fraction  $Y$ . The exact primordial abundances remain a topic of debate with two, largely incompatible, determinations for the helium mass fraction [69, 70, 71, 72, 73] and excessive scatter in the measurements of deuterium [14, 74] but these two nuclei still represent the best probes of BBN.

The error in the observed helium-4 mass fractions are 2% for  $Y_{OSW}$ , 1% for  $Y_{IT}$  which compares well with the spread in the predicted mass fraction plotted in figure (8). We can integrate over the possible values for the prediction, at a fixed  $\eta$  and  $B_{2_n}$ , using the distributions found earlier, and find

$$\mathcal{L}(\eta, B_{2_n}|\hat{\mathbf{Y}}) = \frac{1}{\sqrt{2\pi|V|}} \times \exp\left[-\frac{1}{2}(\hat{\mathbf{Y}} - \mathbf{Y})^T V^{-1} (\hat{\mathbf{Y}} - \mathbf{Y})\right], \quad (20)$$

where  $\hat{\mathbf{Y}}$  denotes the vector whose elements are the observations and  $\mathbf{Y}$  the vector whose elements are the predictions and  $V$  is the covariance matrix - the sum of the (diagonal) covariance matrix for the observations,  $V_O$ , and the two covariance matrices  $V_R$  and  $V_S$ . Contours of the likelihood are shown in figure (12) which shows that the use of deuterium and helium-4 breaks the degeneracy seen in each separately, and, indeed, the limits to the dineutron binding energy are independent of the baryon-to-photon ratio.

Marginalizing over the baryon-to-photon ratio,  $\eta$ , we obtain the results shown in figure (13). The two upper limits for  $B_{2_n}$  are not greatly influenced by the different

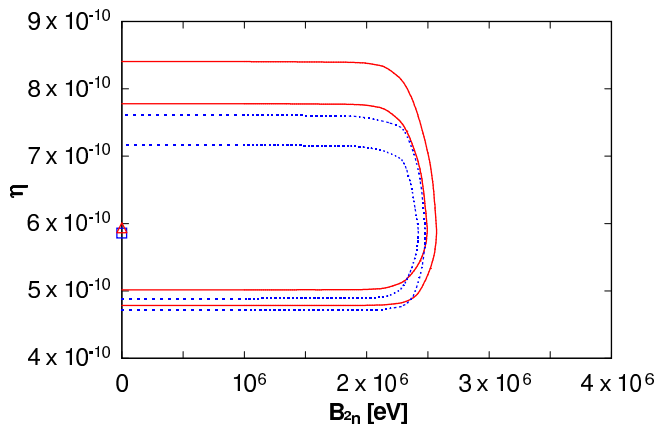


FIG. 12: The 95% and 99% confidence contours using the Olive, Steigman and Walker (solid curves) and Izotov and Thuan (dashed curves) helium-4 mass fractions observations and the Barger *et al.* [14] primordial deuterium abundance. The best fit points, both at  $B_{2n} = 0$ , are denoted by the triangle for OSW, the square for IT.

primordial helium-4 mass fractions found in the literature.

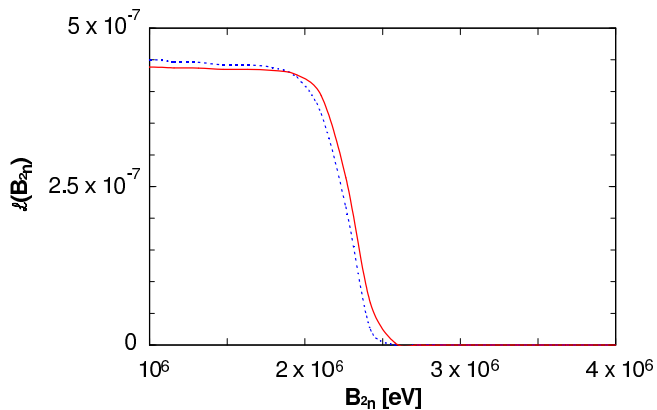


FIG. 13: The marginalized likelihood function for  $B_{2n}$  using the Olive, Steigman and Walker (solid curve) and Izotov and Thuan (dashed curve) helium-4 mass fractions observations and the Barger *et al.* [14] primordial deuterium abundance.

## VIII. SUMMARY AND CONCLUSIONS

We have examined the role that a stable dineutron may play in BBN as a function of its binding energy,  $B_{2n}$ , up to 4 MeV. We have estimated the important new reactions that enter into the BBN reaction network and examined, in detail, the change in the nucleon flow. We find that the range  $0 \leq B_{2n} \leq 4$  MeV can be subdivided into three regions:  $B_{2n} \leq B_D$ ,  $B_D \leq B_{2n} \leq 3$  MeV and  $3 \text{ MeV} \leq B_{2n}$ . The boundaries are due to the sign

inversion of the  ${}^2\text{n}(p, n)\text{D}$  and  ${}^3\text{He}({}^2\text{n}, \text{D})\text{T}$  Q-values respectively. Below  $B_D$  the dineutron has little effect upon BBN but as we increased  $B_{2n}$  beyond this value it began to interfere with the nucleon flow between deuterons and tritium. The helium-4 mass fraction increased by  $\sim 10\%$  and the deuterium abundance dropped by  $\sim 40\%$ . Above 3 MeV the nucleon flow settled into a new pattern, the helium-4 mass fraction plateaued to new level and the rate at which the deuterium abundance decreases with  $B_{2n}$  slowed. A small change to the nucleon flow from tritium to helium-4 was seen.

We estimated the error in the predictions by sampling the distribution of abundances when the dineutron reactions were multiplied by random factors and found that the prediction of an increase in the helium-4 mass fraction and decrease in deuterium abundance were reliable. The degeneracy between  $B_{2n}$  and the baryon-to-photon ratio,  $\eta$ , that occurs for  $Y$  and  $\text{D}/{}^1\text{H}$  separately was broken when both were considered simultaneously. We then constructed the 2-D likelihood function  $\mathcal{L}(\eta, B_{2n}|Y, \text{D}/\text{H})$  by using both the OSW [68] and IT [69, 70] helium-4 mass fractions and the Barger *et al.* [14] deuterium abundance and then marginalized over  $\eta$  to derive the likelihood distribution for  $B_{2n}$ . We found that dineutron binding energies above  $\sim 2.5$  MeV could not be accommodated by BBN within both allowed ranges of  $Y$

Throughout our calculation we have only permitted the variation of the dineutron binding energy. In reality, whatever the source of the stability of the dineutron, naively the binding energies of the other nuclei should also change. The range in  $B_{2n}$  we investigated is much larger than the range in  $B_D$  that Kneller & McLaughlin permitted but we notice that the increase in  $Y$  and decrease in  $\text{D}/\text{H}$  seen there when  $B_D$  increased is also mimicked by the dineutron. Thus if  $B_D$  and  $B_{2n}$  increase in tandem then the stability of the dineutron cannot reverse the increase in  $Y$  whatever the relative magnitudes of the two binding energies and even though dineutrons may alter the nucleon flow. If these two binding energies change in opposite senses then the situation is more confused: the effect of a decrease in  $B_D$  is the immediate decrease in the helium-4 mass fraction which may not be reversed by the presence of a stable dineutron unless  $B_{2n} \gtrsim B_D$ . A better understanding of the net effect, and a more concrete limit to the permitted variation of both the deuteron and dineutron binding energies, could be derived if the relationship between them were known and we were not forced to have to treat each as independent. Furthermore, if such a calculation shows that the predicted helium-4 mass fraction can be consistent with observations, without changing the compatibility of  $\eta_{\text{BBN}}$  and  $\eta_{\text{CMB}}$  and the deuterium abundance greatly, then an examination of the effects upon the primordial yield of lithium-7, which, in standard BBN, is overproduced theoretically, would be in order. Although we have not included any dineutron reaction involving nuclei with mass above  $A = 4$ , one can speculate that the omitted reaction  ${}^7\text{Be}({}^2\text{n}, n\alpha){}^4\text{He}$  could play a significant role since

beryllium-7 (before it decays to  ${}^7\text{Li}$ ) is the chief component of the primordial  $A = 7$  isobar yield at  $\eta \sim 6 \times 10^{-10}$ .

In this paper we have shown that the dineutron can become bound at a level up to that of the deuteron without disrupting the standard nuclear flow in BBN or significantly altering predicting BBN abundance yields. Beyond that, changes to the nuclear flow and to predicted abundance yields appear. It is important to note that we have allowed only one parameter, the dineutron binding energy, to vary. Further work on the interdependence of cross sections and binding energies in nuclear theory would be required to reduce the errors presented here and

to make a more concrete connection with the underlying fundamental constants.

### Acknowledgments

The authors would like to thank Eric Braaten for useful discussions. This work was supported by the U.S. Department of Energy under grant DE-FG02-02ER41216.

- 
- [1] D. N. Schramm, *Space Science Reviews*, **84**, 3 (1998)
- [2] E. Vangioni-Flam, A. Coc and M. Cassé, *Nuc. Phys. A*, **718**, 389 (2003)
- [3] G. Steigman, D. N. Schramm and J. R. Gunn, *Phys. Lett. B*, **66**, 202 (1997)
- [4] J. Yang, D. N. Schramm, G. Steigman and R. T. Rood, *Ap. J.*, **227**, 697 (1979)
- [5] E. Lisi, S. Sarkar and F. L. Villante, *Phys. Rev. D*, **59**, 123520 (1999)
- [6] J. P. Kneller *et al.*, *Phys. Rev. D*, **64**, 123506 (2001)
- [7] G. Beaudet and A. Yahil, *Ap. J.*, **218**, 253 (1977)
- [8] R. V. Wagoner, W. A. Fowler and F. Hoyle, *Ap. J.*, **148**, 3 (1967)
- [9] H.-S. Kang and G. Steigman, *Nucl. Phys. B*, **372**, 494 (1992)
- [10] K. Kohri, M. Kawasaki and K. Sato, *Ap. J.*, **490**, 72 (1997)
- [11] K. A. Olive *et al.*, *Phys. Lett. B*, **265**, 239 (1991)
- [12] R. J. Scherrer, *M. N. R. A. S.*, **205**, 683 (1983)
- [13] A. Yahil and G. Beaudet, *A. and A.*, **206**, 415 (1976)
- [14] V. Barger *et al.*, *Phys. Lett. B*, **566**, 8 (2003)
- [15] V. Barger *et al.*, *Phys. Lett. B*, **569**, 123 (2003)
- [16] A. Serna and R. Dominguez-Tenreiro, *Phys. Rev. D*, **48**, 1591 (1993)
- [17] A. Serna, R. Dominguez-Tenreiro and G. Yepes, *Ap. J.*, **391**, 433 (1992)
- [18] R. Bean, S. H. Hansen and A. Melchiorri, *Phys. Rev. D*, **64**, 103508 (2001)
- [19] J.P. Kneller and G. Steigman, *Phys. Rev. D*, **67**, 063501 (2003)
- [20] X. Chen, R. J. Scherrer and G. Steigman, *Phys. Rev. D*, **63**, 123504 (2001)
- [21] R. Foot, *Phys. Rev. D*, **61**, 023516 (2000)
- [22] C. Lunardini and A. Y. Smirnov, *Phys. Rev. D*, **64**, 073006 (2001)
- [23] A. D. Dolgov *et al.*, *Nucl. Phys. B* **632**, 363 (2002)
- [24] Y. Y. Wong, *Phys. Rev. D*, **66**, 025015 (2002)
- [25] K. N. Abazajian, J. F. Beacom and N. F. Bell, *Phys. Rev. D*, **66**, 013008 (2002)
- [26] M. Kaplinghat, G. Steigman and T. P. Walker, *Phys. Rev. D*, **61**, 103507 (2000)
- [27] E. W. Kolb and R. J. Scherrer, *Phys. Rev. D*, **25**, 1481 (1982)
- [28] X. Shi, D. N. Schramm and B. D. Fields, *Phys. Rev. D*, **48**, 2563 (1993)
- [29] X. Shi, G. M. Fuller and K. Abazajian, *Phys. Rev. D*, **60**, 063002 (1999)
- [30] L. Bergstrom, S. Iguri and H. Rubinstein, *Phys. Rev. D*, **60**, 045005 (1999) [arXiv:astro-ph/9902157]
- [31] P.P. Avelino *et al.*, *Phys. Rev. D* **64**, 103505 (2001)
- [32] K. M. Nollett and R. E. Lopez, *Phys. Rev. D*, **66**, 063507 (2002) [arXiv:astro-ph/0204325]
- [33] J. J. Yoo and R. J. Scherrer, [arXiv:astro-ph/0211545]
- [34] V. V. Flambaum and E. V. Shuryak, *Phys. Rev. D*, **65**, 103503 (2002) [arXiv:hep-ph/0201303]
- [35] V. V. Flambaum and E. V. Shuryak, [arXiv:hep-ph/0212403]
- [36] J.P. Kneller and G.C. McLaughlin, to be published in PRD
- [37] J. K. Webb *et al.*, *Phys. Rev. Lett.* **82**, 884 (1999) [arXiv:astro-ph/9803165]
- [38] J. K. Webb *et al.*, *Phys. Rev. Lett.* **87**, 091301 (2001) [arXiv:astro-ph/0012539]
- [39] J. N. Bahcall, C. L. Steinhardt and D. Schlegel, [arXiv:astro-ph/0301507]
- [40] R. H. Phillips and K. M. Crowe, *Phys. Rev.*, **96**, 484 (1954)
- [41] K. Ilakovac *et al.*, *Phys. Rev.*, **124**, 1923 (1961)
- [42] W. R. Gibbs, B. F. Gibson and G. J. Stephenson, *Phys. Rev. C*, **11**, 90 (1975)
- [43] O. Schori *et al.*, *Phys. Rev. C*, **35**, 2252 (1987)
- [44] B. L. Cohen and T. H. Handley, *Phys. Rev.*, **92**, 101 (1953)
- [45] O. V. Bochkarev *et al.*, *JETP Letters*, **42**, 374 (1985)
- [46] O. V. Bochkarev *et al.*, *JETP Letters*, **42**, 377 (1985)
- [47] K. K. Seth and B. Parker, *Phys. Rev. Letts.*, **66**, 2448 (1991)
- [48] F. M. Marques *et al.*, *Phys. Rev. C*, **65**, 044006 (2003)
- [49] S. R. Beane and M. J. Savage, *Nucl. Phys. A*, **713**, 148 (2003) [arXiv:hep-ph/0206113]
- [50] S. R. Beane and M. J. Savage, *Nucl. Phys. A*, **717**, 91 (2003) [arXiv:nucl-th/0208021]
- [51] M. S. Smith, L. H. Kawano and R. A. Malaney, *Astrophys. J. Supp. Series*, **85**, 219 (1993)
- [52] E. Braaten and H. W. Hammer, *Phys. Rev. Lett.* **91**, 102002 (2003) [arXiv:nucl-th/0303038].
- [53] W. A. Fowler, G. R. Caughlan and B. A. Zimmerman, *Ann. Rev. Astron. Astro.*, **5**, 525 (1967)
- [54] G. Gamow, ‘Structure of atomic nuclei and nuclear transformations, being a second edition of Constitution of atomic nuclei and radioactivity’, Oxford, Clarendon Press, (1937).

- [55] H. Bethe, Rev. Mod. Phys., vol 9, 69 (1937)
- [56] D.D. Clayton, 'Principles of stellar evolution and nucleosynthesis', University of Chicago Press, (1983)
- [57] G.S. Chulick *et al.*, Nucl. Phys. A, **551**, 255 (1993)
- [58] <http://www.nndc.bnl.gov/nndc/endl/>
- [59] D.R. Tilley *et al.*, Nucl. Phys. A, **708**, 3 (2002)  
(see also [http://www.tunl.duke.edu/nucldata/HTML/HTML\\_Project.shtml](http://www.tunl.duke.edu/nucldata/HTML/HTML_Project.shtml))
- [60] G. Rupak, Nucl. Phys. A, **678**, 405 (2000)  
[arXiv:nucl-th/9911018]
- [61] A. Cuoco *et al.*, [arXiv:astro-ph/0307213]
- [62] G. Fiorentini, E. Lisi, S. Sarkar and F. L. Villante, Phys. Rev. D, **58**, 063506 (1998)
- [63] L. M. Krauss and P. Romanelli, Astrophys. J., **358**, 47 (1990)
- [64] L. M. Krauss and P. Kernan, Phys. Letts., **B347**, 347 (1995)
- [65] K. M. Nollett, S. Burles, Phys.Rev. D, **61** 123505 (2000)
- [66] J. Bernstein, L. S. Brown and G. Feinberg, Rev. Mod. Phys. **61**, 25 (1989)
- [67] S. Sarkar, 1996, Rep. Prog. Phys., **59**, 1493 (1996)
- [68] K. A. Olive, G. Steigman and T. P. Walker, Phys. Rep., **333**, 389 (2000)
- [69] Y. I. Izotov, T. X. Thuan and V. A. Lipovetsky, ApJSS., **108**, 1 (1997)
- [70] Y. I. Izotov and T. X. Thuan, ApJ., **500**, 188 (1998)
- [71] K. A. Olive and G. Steigman, ApJSS., **97**, 49 (1995)
- [72] K. A. Olive, E. D. Skillman and G. Steigman, ApJ., **483**, 788 (1997)
- [73] B. D. Fields and K. Olive, ApJ, **506**, 177 (1998)
- [74] D. Kirkman *et al.*, [arXiv:astro-ph/0302006]